EPH - International Journal of Applied Science
ISSN (Online): 2208-2182
Volume 05 Issue 03 July 2019

DOI: https://doi.org/10.53555/eijas.v5i3.113

CHARACTERIZATION OF CERTAIN PHYSICAL PROPERTIES ON MODIFIED KAOLINITE-COUPLED CATALYSTS PREPARED WITH AG AND ZN IONS

Shu-Lung Kuo[1], Ching-Lin Ho[2*]
*[1,*2]Department of Technology Management, Open University of Kaohsiung, Taiwan*

Corresponding Author:-

Abstract:-

This study used kaolinite clay as a carrier and exchanged Ag^+ and Zn^{2+} onto the kaolinite via ion exchange. The coupled kaolinite-Ag/Zn catalysts at the nanolevel were formed after surface modification. Various physicochemical experiments, such as Fourier-transform infrared spectroscopy (FT-IR) analysis, x-ray diffraction (XRD) analysis, transmission electron microscopy (TEM) analysis, thermal analysis, and potentiometric titration analysis were conducted to further discuss the physicochemical properties of the kaolinite-Ag/Zn catalysts.

First, a function group analysis on the kaolinite clay conducted using a Fourier-transform infrared spectrometer showed many significant and complex wave crests in the following wavenumber sections of the fingerprint area: 415~600 cm^{-1} and 750~1170 cm^{-1}; these represent strong bonds between impure silicates (Si-O) and silicates (O-Si-O) within the silicate mineral. The mineral structures of the kaolinite-Ag/Zn catalysts remained intact after being sintered at 350°C. In terms of the x-ray diffraction analysis, following high-temperature sintering a dehydration reaction occurred in the kaolinite-Ag/Zn catalysts. The spacing of layers was thereby narrowed to 0.7170 nm. Moreover, a TEM observation of the kaolinite-Ag/Zn catalysts after high-temperature sintering showed that the sizes of Ag^+ and Zn^{2+} on the kaolinite-Ag/Zn catalysts were between 25 and 60 nm, respectively. This proves that with ion exchange, the kaolinite-Ag/Zn catalysts are at the nanolevel. Regarding thermal analysis, the kaolinite-Ag/Zn catalysts had endothermic peaks at 464°C, 527°C and 888°C, respectively and exothermic peaks at 585°C and 921°C, respectively. As for TGA weight loss, two pyrolysis temperatures were found: The first pyrolysis occurred at 464°C, where the weight loss was caused by oxidative pyrolysis. The second pyrolysis occurred at 775°C, where the TGA weight loss resulted from decomposition of the remaining organic (carbon-containing) compounds. Lastly, regarding potentiometric titration, there were two end points of the titration for the kaolinite-Ag/Zn catalysts, indicating that there are two different acidic function groups. The titration curves of these said end points were obviously affected by two ions, and these two end points of the titration were quite obvious. The intensities of the two acidic function groups were similar; consequently, there is an obvious two-stage dissociation in the titration curves.

Key words:- *Kaolinite, clay, coupled catalysts, x-ray diffraction, thermal analysis*

INTRODUCTION

During the last decade, photocatalyses are becoming more popular to draw significant global interest (Chen et al., 2009). Titanium dioxide (TiO_2) is the most widely used catalyst; it is considered to be an ideal catalyst for photocatalytic oxidation applications (Mo et al., 2009; Chen et al., 2010; Zhong et al., 2010). Numerous reports on the mechanisms of photocatalytic process for disinfecting air have been publishedinliterature(Salvad-Estivilletal.,2007; Mo et al., 2009; Chen et al., 2010). However, not much research has been carried out on the photocatalytic disinfection of airborne bacteria in polluted indoor air despite its capacity and great potential to protect public health.

As the best known photocatalyst, TiO_2 has attracted more attention and interest of many researchers due to its exceptional properties, such as high refractive index and ultraviolet (UV) absorption, excellent incident photoelectric conversion efficiency and dielectric constant, good photocatalytic activity, photostability, chemical stability, and long-time corrosion resistance as well as nontoxicity (Spadavecchia et al., 2014; Yamada et al., 2013; Angelis et al., 2014; Zheng et al., 2013). It has been widely used to solve a variety of environmental problems for the water and soil-based solution utilization.

This study used kaolinite clay as its main catalyst carrier and exchanged Ag^+ and Zn^{2+} onto the catalyst carrier; the coupled kaolinite-Ag/Zn catalysts were formed after high-temperature sintering. Various experimental methods, such as Fourier-transform infrared spectroscopy (FT-IR) analysis, x-ray diffraction (XRD) analysis, transmission electron microscopy (TEM) analysis, differential thermal scanning calorimetry analysis, thermogravimetric analysis, and potentiometric titration analysis, were adopted to explore various physical and chemical properties of the kaolinite-Ag/Zn catalysts.

1. Materials and methods

1.1 The purification and preparation of sodium saturated kaolinite

60 g of commercially available kaolinite are placed in a 2-liter beaker, and 1.8 liters of deionized water are added to it. After stirring, it is soaked for days to fully expand it. After it is expanded, 250 ml of the kaolinite suspension are taken out of the beaker. Sand is filtered using the wet sieving method with a 300-mesh sieve; the filtrate is transferred to a 1-liter sedimentation cylinder, and deionized water is added to make up the full 1 liter capacity. It is then left to naturally sediment after being stirred rigorously with a stirring rod. The suspension at the top of the sedimentation cylinder is then siphoned by 10 cm 8 h later. An 18000 rpm high-speed centrifuge is used to centrifuge the suspension. Sodium saturation of the kaolinite obtained after centrifugation is performed with 1 M NaCl solution. Next, the saturated kaolinite is ground into powder with an agate mortar after freeze drying it to obtain the sodium saturated kaolinite.

1.2 Preparation of kaolinite-Ag/Zn catalysts

Formulate 58 ml of 0.1 N $AgNO_3$ and 42 ml of 0.1 N $ZnCl_2$, respectively. 2% of sodium saturated kaolinite is added, and then stirred for 48 h using the water bath method to keep the temperature at 40°C. Next, it is stirred evenly for 2 h at 80°C. It is then left and the supernatant removed. A50% ethanol solution is used to remove the chlorine ions. The modified kaolinite-Ag/Zn catalysts are dried using freeze drying. After these are removed and ground, they are sintered in a high-temperature furnace at 350°C for 2 h. These are saved for later use once they have reached room temperature. The concentrations of Ag and Zn in the prepared catalysts are the same.

1.3 X-ray Diffraction Analysis (XRD Analysis)

X-ray Diffraction Analysis utilizes the X-ray Diffractometer coded with Rigaku RINT 200 to conduct the analysis. The CuK_α is used as a photo source to separately analyze the crystalline forms of kaolinite-Ag/Zn catalysts after modification in order to explore spacing of layers for these materials. The wavelength of the X-ray produced for testing operational current is 1.5418 $_A^O$ and 10 mA, with 20kV fr voltage, a 5 deg/min scanning rate and a scanning angle of $2\theta=2\sim40^o$.

1.4 Fourier-transfer infrared spectrometer- Function Group Authentication

A Fourier-transfer infrared spectrometer (FT-IR) is adopted for analysis to make use of the movement or vibration of molecular structure to absorb radiation with the same frequency. The fingerprint area and Eigen-area of FT-IR are used for determination of the homeotype substitution of clay catalyst and the existence of organic molecules.

The kaolinite-Ag/Zn and KBr powder is placed in the oven separately to dry for 48 h, and then mixed in a 1:10 ratio, before being ground in an agate mortar. An oil presser using a pressure of 10 tons is used to produce a transparent sheet which is then scanned from 4000 cm^{-1} to 400 cm^{-1} for analysis on the spectrometer.

1.5 Transmission Electron Microscopy (TEM) Analysis

Using a transmission electron microscope, the size of kaolinite-Ag/Zn catalysts and their distribution was observed. The microscope model used was HR-TEM 2100 with the emitting energy coming from a field emission filament with high space and energy resolution.

1.6 Thermal analysis

This study used a differential thermal scanning calorimeter and a thermogravimetric analyzer (DSC-TGA), to conduct thermal analysis of kaolinite-Ag/Zn catalysts at different rates of temperature increase. DSC-TGA, manufactured by the US TA-Instrument, is capable of measuring the changes of solid, powder, gum, and liquid material at high temperatures. The analysis steps are as follows: (1) Sample preparation: Testing samples of kaolinite-Ag/Zn catalysts are ground into fine powder by agate mortar and dried. About 5-20 mg of the samples is placed on the platinum pan for measurement. (2) Analysis condition: Nitrogen is used as purge gas at the rate of 10°C/min of temperature increase. With a temperature

sweep range of between 40ºC and 1200ºC, it measures the heat stability, the curve of heat difference, and the loss of weight in the samples.

1.7 Potentiometric titration analysis

Potentiometric titration primarily uses changes in the electrode potentials of solutions to represent changes in titration curves. It also uses changes in pH values to observe the properties of acidic function groups. The steps for the experiment are as follows: 0.3 g kaolinite-Ag/Zn catalysts are put into a beaker, and 300 mL of deionized water are added.
Acidify 0.1 M HNO_3 to pH3. Add 0.2 mL of a 0.1 M concentration of NaOH solution each time to perform the titration. Changes in pH values and electric potentials are recorded after approximately 5 minutes when the titration is stabilized; recording is continued until reaching pH11.

2. Results and discussion

2.1 Results of XRD analysis

Figure 1 shows the XRD analysis results of the sodium-saturated kaolinite before sintering. Figure 2 shows the XRD analysis results of the kaolinite-Ag/Zn catalysts sintered at 350ºC.
As kaolinite contains minimal amounts of quartz (2θ is about 37.7 º) and mica (2θ is about 24.9 º), calculation done using Bragg's law: $2d\sin\theta=n\lambda$ suggests that before the kaolinite is modified, the spacing of layers for sodium saturated kaolinite at room temperature is 0.7177 nm. After it is modified by Ag^+ and Zn^{2+} and sintered at 350ºC, the spacing of layers for the kaolinite Ag/Zn catalysts narrows to 0.7170 nm. The kaolinite is a 1:1 type clay mineral; its plasticity, viscosity, shrinkage and expansion are relatively weak. It is a non-expansion crystal lattice. Due to incomplete bonding between thin films of the kaolinite (thin films of lamella crystal), the spacing of layers for the aquifer with single molecules is narrowed after being modified by Ag^+ and Zn^{2+} and sintered, whereby water evaporates from boiling.

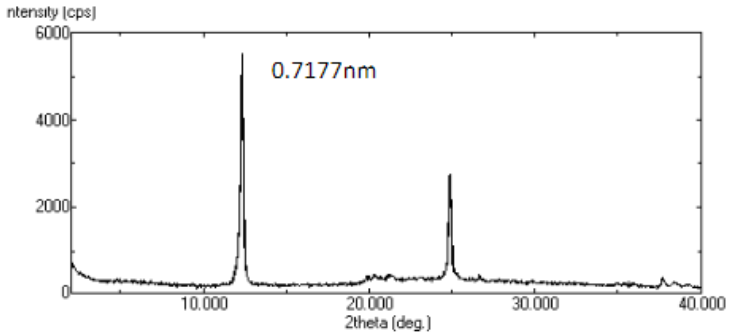

Figure 1. XRD analysis of the kaolinite (before being sintered at high temperatures)

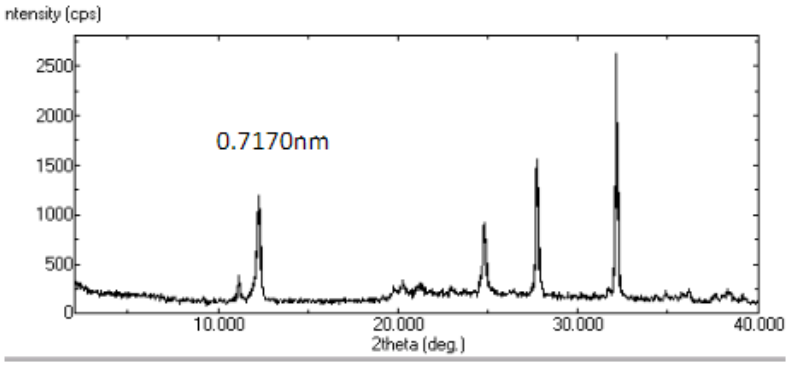

Figure 2. XRD analysis of the kaolinite-Ag/Zn catalysts (sintered at 350ºC)

2.2 Results of FT-IR analysis

Figures 3 and 4 show FT-IR spectrums of the kaolinite and the kaolinite-Ag/Zn catalysts, respectively. Figure 3 shows many significant and complex wave crests in the following wavenumber sections in the fingerprint area: 415~600 cm^{-1} and 750~1170 cm^{-1}; these represent strong bonds between impure silicates (Si-O) and silicates (O-Si-O) within the silicate mineral. There are also -OH absorption peaks in the following wavenumber sections: 3300^{-1}~3700 cm^{-1}. However, since the kaolinite is a 1:1 type clay mineral, it barely has the function of isomorphous replacement. Figure 4 shows that the structure of the coupled kaolinite-Ag/Zn catalysts remains intact after being sintered at 350ºC for 2 h; it still keeps the absorption band of clay minerals with inherent characteristics. As such, a catalyst carrier will still have a good clay structure via complex modification and sintering, whereby it can be used as a photocatalyst (Doong et al., 2001).

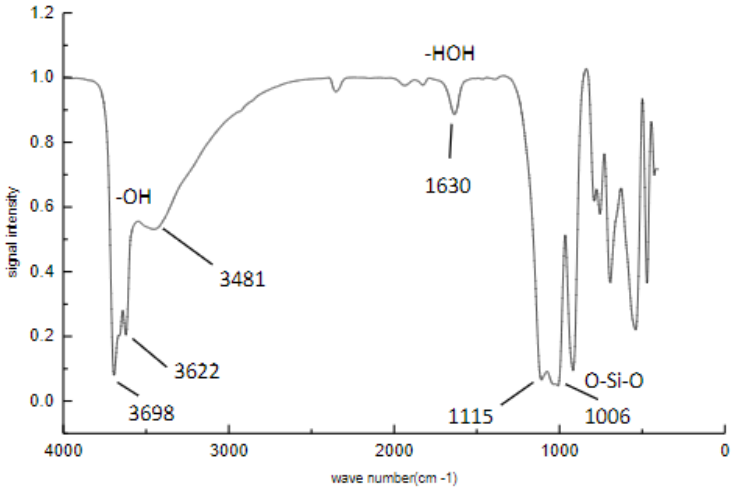

Figure 3. FT-IR spectrums of the kaolinite (before being sintered at high temperature)

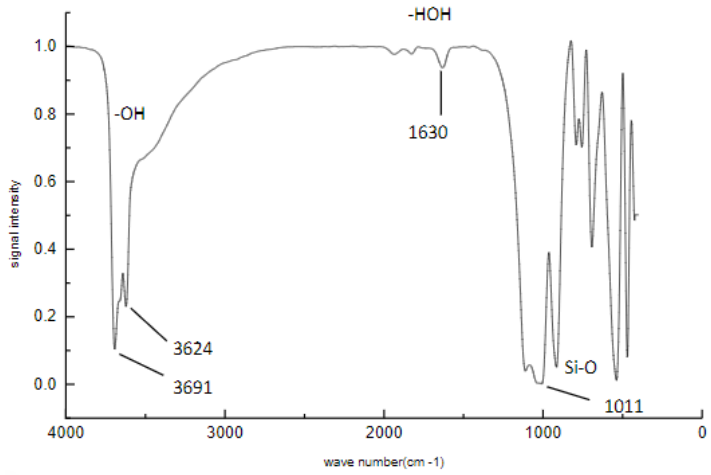

Figure 4. FT-IR spectrums of the kaolinite-Ag/Zn catalysts (sintered at 350ºC)

2.3 Results of TEM analysis

Figures 5(a) and 5(b) show the structural patterns of the kaolinite before being sintered. Figure 5(b) shows that the crystalline particles of the kaolinite comprise small sheet-shaped mineral crystals; they are presented as a hexagonal bluff body (hexagonal sheet-shaped crystals). With diameters between 200 nm and 500 nm, these crystalline particles cannot be easily broken into smaller and thinner crystals, and thus possess good crystallinity. Figure 5(c) shows the modified kaolinite-Ag/Zn catalysts; those darker granules are Ag^{+}, and the light-colored ones are Zn^{+}. As shown in the Figure, the distributions of Ag^{+} and Zn^{+} are quite even and intensive. The above TEM analysis results verify that sizes of ions of the modified kaolinite-Ag/Zn catalysts are indeed at the nanolevel. Figure 6 shows the distribution of the kaolinite-Ag/Zn elements identified using an energy dispersive spectrometer (EDS). As shown in the Figure, after being modified by Ag^{+} and Zn^{2+}, the Ag^{+} and Zn^{2+} contents in the kaolinite-Ag/Zn catalysts show certain proportions, indicating that the modified kaolinite-Ag/Zn catalysts indeed have the characteristics of coupled catalysts at the nanolevel.

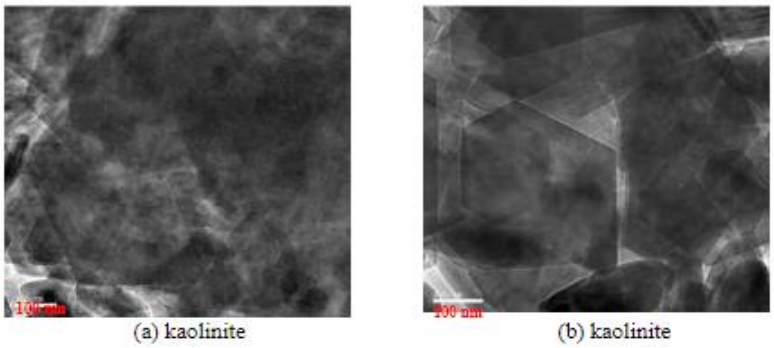

(a) kaolinite (b) kaolinite

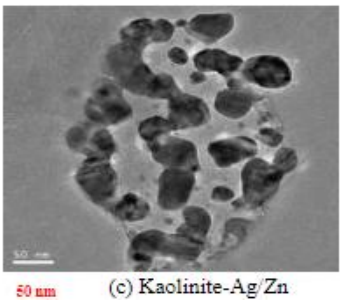

Figure 5. TEM analysis of the kaolinite and kaolinite-Ag/Zn catalysts

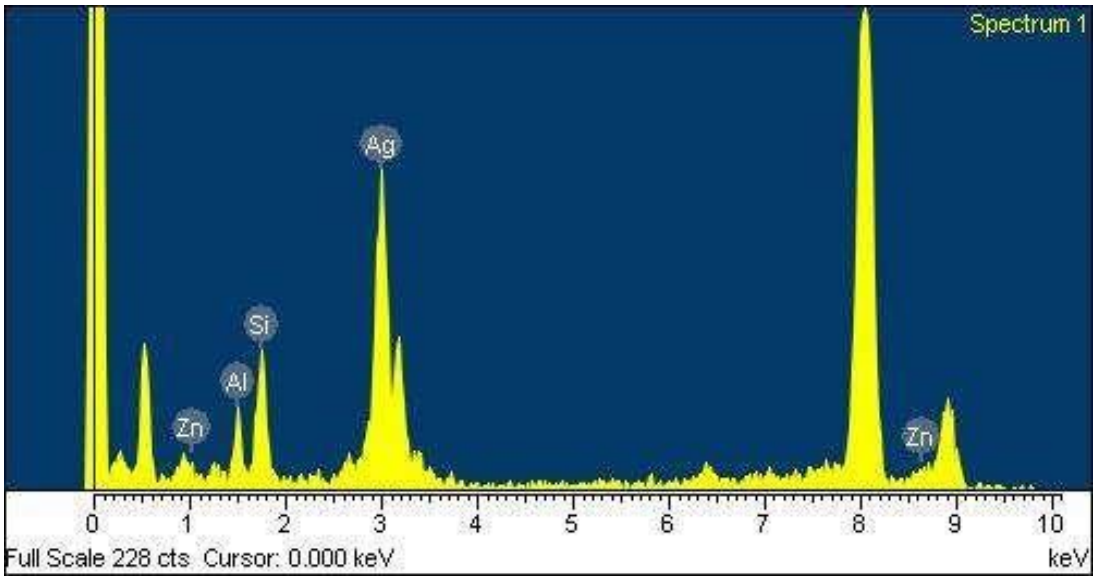

Figure 6. EDS analysis results of the kaolinite-Ag/Zn catalysts

2.4 Result of thermal analysis

Figures 7 and 8 show the results of an analysis on the kaolinite and kaolinite-Ag/Zn catalysts conducted using a differential thermal scanning calorimeter, and a thermogravimetric analyzer (DSC-TGA) in a nitrogen atmosphere with the temperature rising at 10ºC/min (from 40ºC to 1200ºC). As illustrated by the thermal curves in Figure 7, the kaolinite has endothermic peaks (melting peaks) at 77ºC, 530ºC and 1051ºC, respectively; it has exothermic peaks at 583ºC and 1009ºC, respectively. The aforementioned multiple melting peaks suggest that the kaolinite itself has various crystal structures and micro-phase patterns. Moreover, they also suggest that some unstable crystals of the kaolinite itself will melt at a lower temperature during the heating and melting process; they will then form more perfect crystals. These more perfect crystals will melt again as the temperature keeps rising, eventually forming multiple melting peaks (Cho et al., 2004). Thermal analysis results suggest that the kaolinite loses 11.8% of its weight between 425ºC~583ºC. There are smaller changes in its weight loss under 425ºC and above 583ºC. The weight loss transpires along with the occurrence of the endothermic peak at 530ºC, which is a result of the dehydration of hydrate of the kaolinite. There is a higher possibility that weight loss will occur around 530ºC.

Later the kaolinite will undergo a phase transition and turn into metakaolin. The exothermic peak that occurs at 1009ºC happens as the metakaolin undergoes a phase transition and turns into the primary mullite and where the glass phase occurs. In this study, the primary mullite was formed at a temperature higher than 980ºC proposed by Chakraborty and Ghosh (1978); this is because differences in the crystallinity of the kaolinite and the impurities it contains can further affect the temperature at which the primary mullite is formed. Figure 7 also shows a pyrolysis occurred at 425ºC~583ºC, where the weight loss was approximately 11.8%. The exothermic peak at 583ºC was likely caused by the effect of the kaolinite itself. This temperature marks the end point of the major weight loss. As such, it can be inferred that the exothermic peaks which occurred between 583ºC and 1009ºC are where the metakaolin underwent a phase transition and turned into the primary mullite. The increase in weight loss has slowed down in this temperature range.

In terms of the kaolinite-Ag/Zn catalysts, Figure 8 shows that they have endothermic peaks at 464ºC, 527ºC and 888ºC, respectively, and exothermic peaks at 585ºC and 921ºC, respectively. In regard to TGA weight loss, two pyrolysis temperatures are shown in Figure 8: The first pyrolysis occurred at 464ºC, where the weight loss was caused by oxidative pyrolysis. The second pyrolysis occurred at 775ºC, where the TGA weight loss resulted from the decomposition of the remaining organic (carbon-containing) compounds. During the first pyrolysis, the TGA weight loss from 464ºC to 775ºC is estimated to be about 12.2%. During the second pyrolysis, the TGA weight loss from 775ºC to 890ºC is estimated to be about 4.2%. As shown in Figure 8, the weight loss occurred along with the occurrence of the endothermic peak at

527°C, which is related to the dehydration of hydrate of the kaolinite. The kaolinite will later undergo a phase transition and turn into metakaolin. Compared with the temperature of the kaolinite, there will be 2°C delay in the exothermic peak at 585°C, where the metakaolin undergoes a phase transition and turns into the primary mullite (at about 921°C); the increase in weight loss also slows down. Moreover, the primary mullite is formed from the kaolinite-Ag/Zn catalysts at a temperature higher than the 980°C proposed by Chakraborty and Ghosh (1978). As such, it can be inferred that if there is Zn^{2+} exchanged onto the kaolinite, differences in the crystallinity of the kaolinite will affect the temperature at which the primary mullite is formed.

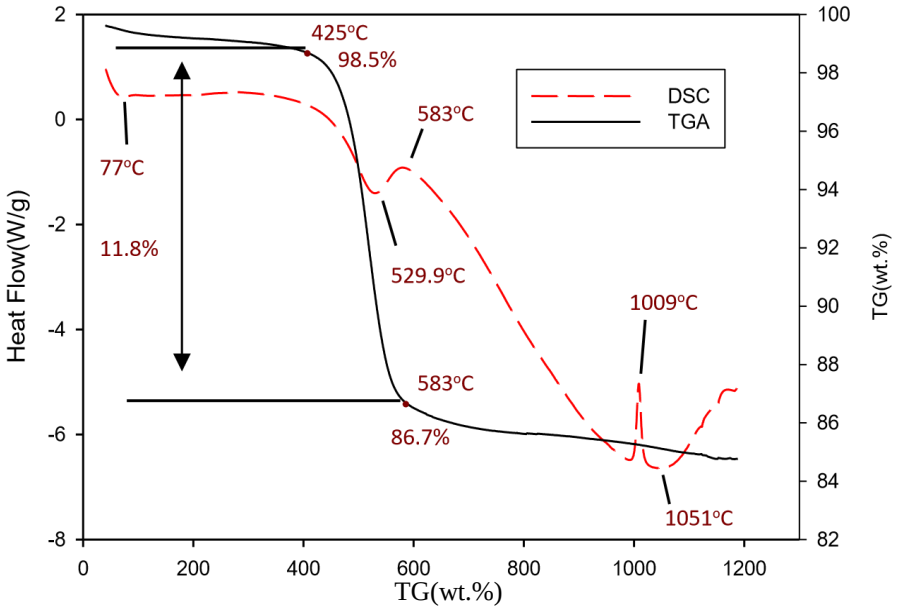

Figure 7. DSC and TGA analyses of the kaolinite

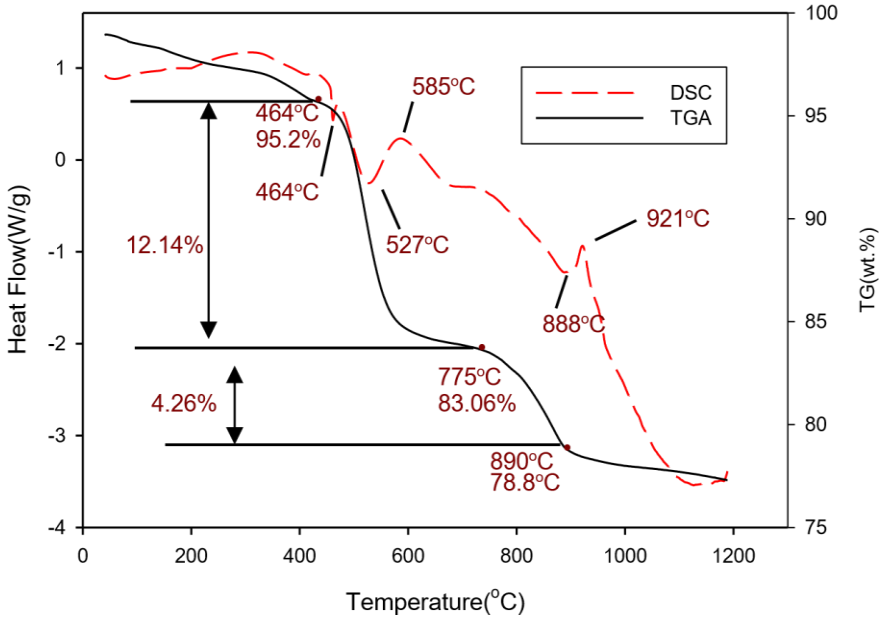

Figure 8. DSC and TGA analyses of the kaolinite-Ag/Zn catalysts

2.5 Potentiometric titration analysis

Figure 9 shows the potentiometric titration curves of the kaolinite and kaolinite-Ag/Zn catalysts. An observation shows that changes in pH values are steeper when the kaolinite approaches the equivalence point, whereas the titration curves of the kaolinite-Ag/Zn catalysts are more moderate. The pH value is approximately 7 when the kaolinite reaches the equivalence point, indicating a neutral state. With 4.2 mL of NaOH, the end point of the titration for the kaolinite can be reached; with approximately 5.2 mL of NaOH, the end point of the titration for the kaolinite-Ag/Zn catalysts can be reached. The above analysis shows that under normal neutral environmental conditions, the ion exchange method can be used to synthesize the kaolinite-Ag/Zn catalysts with powerful catalytic function. Figure 10 shows the function obtained by differentiating changes in potentials caused by NaOH per unit volume; the maximum value is the end point of the titration (equivalence point). As shown in Figure 10, there is only one end point of the titration for the kaolinite, i.e. only one acidic function group. This indicates that either the structure of the kaolinite itself has less acidic function groups, or its acidic function groups are not strong, whereby the presentation of the end point of the titration is also not strong. There are two end points of the titration for the kaolinite-Ag/Zn catalysts, which means that there are two different acidic function groups. This indicates that the two titration curves of the kaolinite-Ag/Zn catalysts are obviously affected by two

ions (Ag^+ and Zn^{2+}). The end points of the titration for these two titration curves are quite obvious. The intensities of the two acidic function groups are similar; consequently, there is an obvious two-stage dissociation in the titration curves.

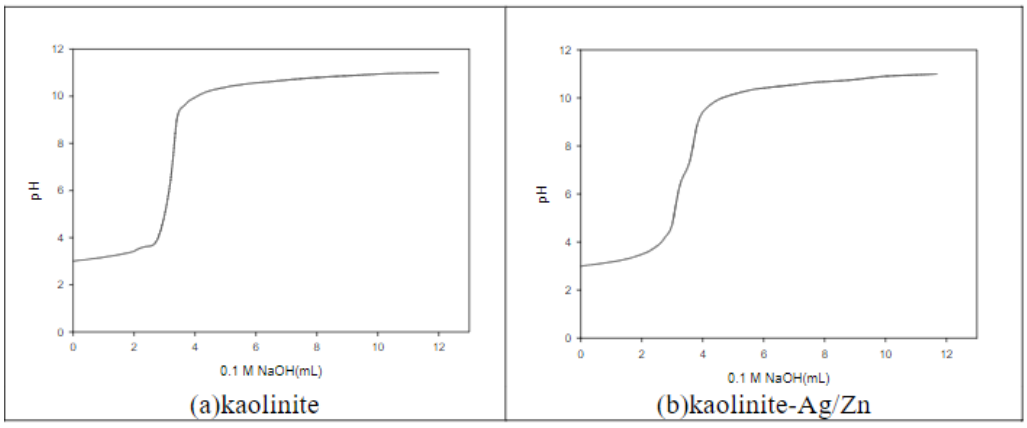

Figure 9. The titration curves of the kaolinite and kaolinite-Ag/Zn catalysts

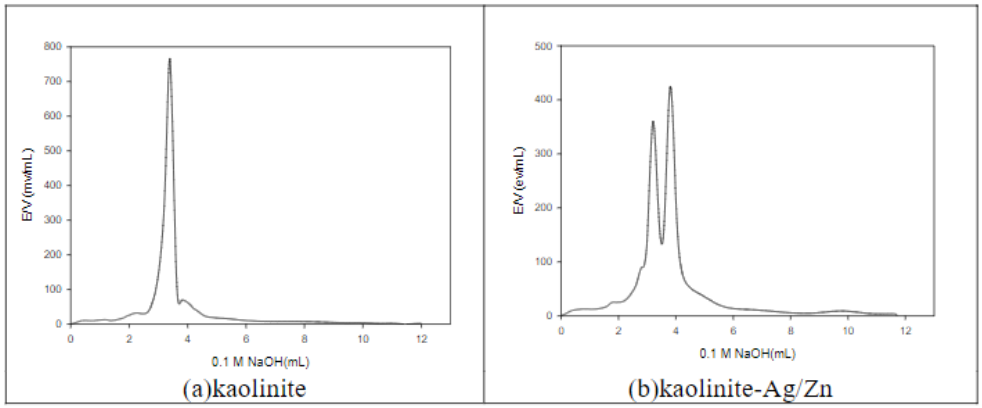

Figure 10. The first derivative of the titration curves of the kaolinite and Kaolinite-Ag/Zn catalysts

3. Conclusion

In this study, the x-ray diffraction analysis showed that the kaolinite contains minimal amounts of quartz (2θ is about 37.7º) and mica (2θ is about 24.9 º). The spacing of layers for the coupled kaolinite-Ag/Zn catalysts was narrowed to 0.7170 nm from 0.7177 nm (the spacing of layers for the kaolinite) after the kaolinite was modified by Ag^+ and Zn^{2+} and sintered at 350ºC. This indicates that a dehydration reaction occurs in the kaolinite-Ag/Zn catalysts after they are heated with spacing of the layers narrowed as a result. An analysis on the modified kaolinite-Ag/Zn catalysts via FT-IR spectrums showed that their mineral structures remain intact; they still keep the absorption band of clay minerals with inherent characteristics. The TEM analysis results verify that sizes of individual Ag and Zn catalyst particles of the kaolinite-Ag/Zn catalysts are indeed at the nanolevel. The Ag^+ and Zn^{2+} contents identified using an energy dispersive spectrometer (EDS) show certain proportions, indicating that the modified kaolinite-Ag/Zn catalysts indeed have the characteristics of coupled catalysts at the nanolevel. As illustrated by the thermal curves, the kaolinite has endothermic peaks (melting peaks) at 77ºC, 530ºC and 1051ºC, respectively, and exothermic peaks at 583ºC and 1009ºC, respectively. In regard to TGA weight loss of the kaolinite-Ag/Zn catalysts, two pyrolysis temperatures were found: The first pyrolysis occurred at 464ºC, where the weight loss is caused by oxidative pyrolysis. The second pyrolysis occurred at 775ºC, where the TGA weight loss results from the decomposition of the remaining organic (carbon-containing) compounds. The aforementioned multiple melting peaks suggest that the kaolinite itself has various crystal structures and micro-phase patterns. Lastly, there are two end points of the potentiometric titration for the kaolinite-Ag/Zn catalysts, meaning that there are two different acidic function groups. The titration curves of the said end points are obviously affected by two ions (Ag^+ and Zn^{2+}), and these two end points of the titration are quite obvious. The intensities of the two acidic function groups are similar; consequently, there is an obvious two-stage dissociation in the titration curves.

References

[1].Angelis, F.D., Valentin, C.D., Fantacci, S., Vittadini, A., Selloni, A. (2014). Theoretical studies on anatase and less common TiO_2 phases: Bulk, surfaces, and nanomaterials. Chem. Rev., 114, 9708-9753.

[2].Chakraborty, A. K., Ghosh, D.K. (1978). Reexamination of kaolinite-to-mullite reaction series. J. Am. Ceram. Soc. 61, 170-178.

[3].Chen, F., Yang, X., Xu, F., Wu, Q., Zhang, Y. (2009). Correlation of photocatalytic bactericidal effect and organic matter degradation of TiO_2 part 1: observation of phenomena. Environ. Sci. Technol. 43, 1180-1184.

[4].Chen, F., Yang, X., Mak, H.K.C., Chan, D.W.T. (2010). Photocatalytic oxidation for antimicrobial control in built environment: A brief literature overview. Build. Environ. 45, 1747-1754.
[5].Cho, M., H. Chung, W. Choi, Yoon, J. (2004). Linear correlation between inactivation of E. coli and OH radical concentration in TiO_2 photocatalytic disinfection. Water Research 38, 1069-1077.
[6].Doong, R. A., C. H. Chen, R. A. Maithreela, Chang, S. M. (2001). The Influence of pH and cadmium sulfide on the photocatalytic degradation of 2-Chlorophenol in titanium dioxide suspensions. Water Research 35, 2873-2880.
[7].Mo, J., Zhang, Y., Xu, Q., Lamson, J.J., Zhao, R. (2009). Photocatalytic purification of volatile organic compounds in indoor air: a literature review. Atmos. Environ. 43, 2229-2246.
[8].Salvad-Estivill, I., Hargreaves, D.M., Puma, G.L. (2007). Evaluation of the intrinsic photocatalytic oxidation kinetics of indoor air pollutants. Environ. Sci. Technol. 41, 2028-2035.
[9].Spadavecchia, F., Ceotto, M., Presti, L. L., Aieta, C., Biraghi, I., Meroni, D., Ardizzone, S., Cappelletti, G. (2014). Second generation nitrogen doped titania nanoparticles: A comprehen- sive electronic and microstructural picture. Chin. J. Chem. 32, 1195-1213.
[10]. Yamada, N., Suzumura, M., Koiwa, F., N. egishi. N. (2013). Differences in elimination efficiencies of Escherichia coli in freshwater and seawater as a result of TiO_2 photocatalysis. Water Res., 47, 2770-2776.
[11]. Zhong, L., Haghighat, F., Blondeau, P., Kozinski, J. (2010). Modeling and physical interpretation of photocatalytic oxidation efficiency in indoor air applications. Build. Environ. 45, 2689-2697.
[12]. Zheng, Z., Zhao, J., Yuan, Y., Liu, H., Yang, D., Sarina, S., Zhang, H., Waclawika, E. R., Zhu, H. (2013). Tuning the surface structure of nitrogen-doped TiO_2 nanofibres- An effective method to enhance photocatalytic activities of visible-light-driven green synthesis and degradation. Chem. Eur. J. 19, 5731-5741.